Molecular Engineering of Fluorene-Based Hole Transporting Materials for Efficient Perovskite Solar Cells

Aistė Jegorovė[†,1], Cristina Momblona[†,2], Marytė Daškevičienė[1], Artiom Magomedov[1], Rimgaile Degutyte[3], Abdullah M. Asiri[4], Vygintas Jankauskas[5], Albertus Adrian Sutanto[2], Hiroyuki Kanda[2], Keith Brooks[2], Nadia Klipfel[2], Mohammad Khaja Nazeeruddin,[2]* Vytautas Getautis[1]*

[1]Department of Organic Chemistry, Kaunas University of Technology, Kaunas LT-50254, Lithuania.

[2]Group for Molecular Engineering of Functional Material, Institute of Chemical Sciences and Engineering, École Polytechnique Fédérale de Lausanne, CH-1951 Sion, Switzerland.

[3]Department of Food Science and Technology, Kaunas University of Technology, Kaunas LT-50254, Lithuania.

[4]Center of Excellence for Advanced Materials Research (CEAMR), King Abdulaziz University, P.O. Box 80203, 21589 Jeddah, Saudi Arabia.

[5]Institute of Chemical Physics, Vilnius University, Vilnius LT-10257, Lithuania.
E-mail: mdkhaja.nazeeruddin@epfl.ch, vytautas.getautis@ktu.lt.

Keywords: hole transporting materials, fluorene, carbazolyl chromophores, spiro-OMeTAD analogues, perovskite solar cells.

New Spiro-OMeTAD analogues and the simpler "half" structures with the terminated methoxyphenyl and/or carbazolyl chromophores were successfully synthesized under Hartwig-Buchwald amination conditions using commercially available starting materials. New fluorene-based hole transporting materials (HTMs) combined with suitable ionization energies properly align with the valence band of the perovskite absorber. Additionally, these compounds are amorphous, what is an advantage for the formation of homogenous films, as well as eliminates

possibility for films to crystallize during operation of the devices. The most efficient PSCs perovskite devices contained carbazolyl-terminated Spiro-OMeTAD analogue **V1267** and reached a PCE of 18.3 %, along with a short-circuit current density (J_{SC}), open-circuit voltage (V_{OC}), and fill factor (*FF*) of 23.41 mA cm^{-2}, 1.06 V, and 74.0 %, respectively. Moreover, "half" structures with methoxyphenyl/carbazolyl fragments show excellent long-term stability and outperform Spiro-OMeTAD, and, therefore, hold a great prospect for practical wide-scale applications in optoelectronic devices.

1. Introduction

Perovskite solar cells (PSCs) have recently emerged as a promising technology for the further cost reduction of the energy production from the sunlight. Starting from the first publication by A. Kojima et al. back in 2009,[1] PCSs have reached 25.5% efficiency of the single-junction devices,[2] and over 29% efficiency of the Silicon/perovskite tandem devices.[3] The advantage of the PSCs over traditional solar cell technologies lays in the vast variety of the available deposition techniques, such as solution-processing (e.g. inject-printing,[4] slot-die,[5] blade-coating[6] etc.) and vapor deposition.[7-9] Moreover, over the years several different architectures of the devices have been investigated (e.g. n-i-p or "regular", p-i-n or "inverted", mesoscopic),[10, 11] which further increases attractiveness of this technology.

The main reason behind the rapid progress of the PSCs mostly comes from the optimization of the perovskite absorber layer, starting from the deposition methods,[12] advancing to the composition optimization,[13] and finally shifting the focus to the interfaces.[14] However, the progress also strongly depends on the other components of the PSCs, such as electron and hole-selective contacts.[15-19] In particular, use of the modern synthetic methods opens a way for a huge variety of the organic hole transporting materials, while systematic study of variations could lead to the innovations in the field of molecular electronics.[20-24]

Carbazole and fluorene chromophores are among the most popular structural building blocks, used for the construction of the organic hole-transporting materials (HTMs).[25-30] In a recent work it was shown, that the replacment of the methoxyphenyl fragment of the popular HTM Spiro-OMeTAD with the 9,9-dimethylfluorenyl chromophore led to the superior performance.[31] Such an increase in the efficiency and stability was attributed to the optimized thermal properties, as well as beneficial alignment of the energy levels. Moreover, the advantage of carbazole-based HTMs could be the absence of methoxy substituents, such as the

ones found on Spiro-OMeTAD. In this case the hydrophobicity of HTM layer is expected to increase, thus positively affecting the device stability.[32]

In this work, we have investigated Spiro-OMeTAD analogues, in which the methoxyphenyl groups were replaced by carbazolyl chromophores. Thermal, optical, and electrical properties of these compounds are compared to those of the Spiro-OMeTAD. In addition, materials with simpler, "half"- structures were investigated, where 9,9-positions of the central fluorene fragment are occupied by different alkyl chains. Finally, new compounds were investigated in the n-i-p PSCs. The new spiro-OMeTAD analogues present high efficiencies exceeding 17%. The devices fabricated with methoxyphenyl and carbazolyl or only carbazolyl groups achieve high efficiencies of 15-16% and 17-18% PCE respectively. The methoxyphenyl/ carbazolyl-based devices demonstrate excellent stability.

2. Results and discussion

2.1. Synthesis

For the synthesis of new hole transporting materials, used in this study, Buchwald-Hartwig amination reaction conditions were utilized. Spirobifluorene derivatives were synthesized using commercially available 2,2′,7,7′-tetrabromo-9,9′-spirobifluorene as a precursor (**Scheme 1**), while for the "half" compounds, 2,7-dibromofluorene, alkylated with various aliphatic chains was used (**Scheme 2**). These starting materials were coupled with 9-ethyl-*N*-(4-methoxyphenyl)-9*H*-carbazol-3-yl-amine to give target compounds **V1222, V1226**, **V1238**, **V1240** and bis(9-ethyl-9*H*-carbazol-3-yl)amine, to give **V1257, V1258, V1267**, **V1269**. Overall, this relatively simple synthetical strategy gives an opportunity to obtain series of compounds that can be evaluated for their possible application in the PSCs. Detailed synthetic procedures and methods, used to get target and precursor compounds, as well as their detailed structural characterizations are given in Supporting information.
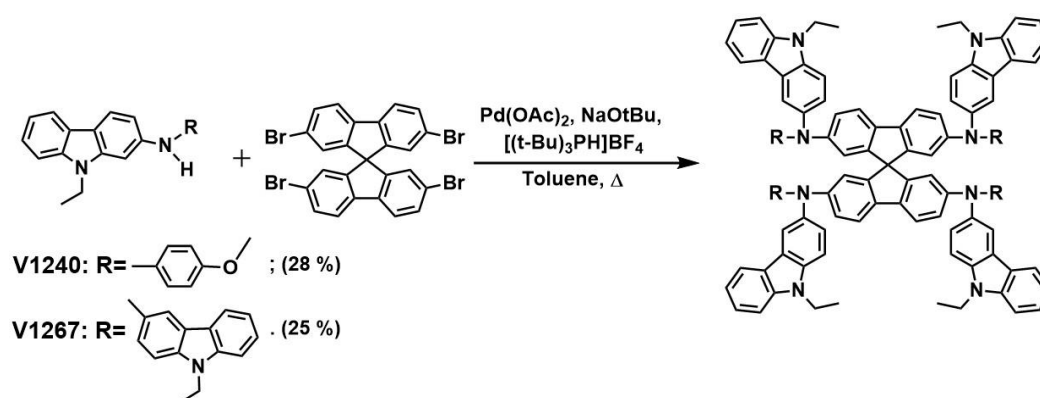
Scheme 1. Synthesis of the spirobifluorene derivatives **V1240** and **V1267**.
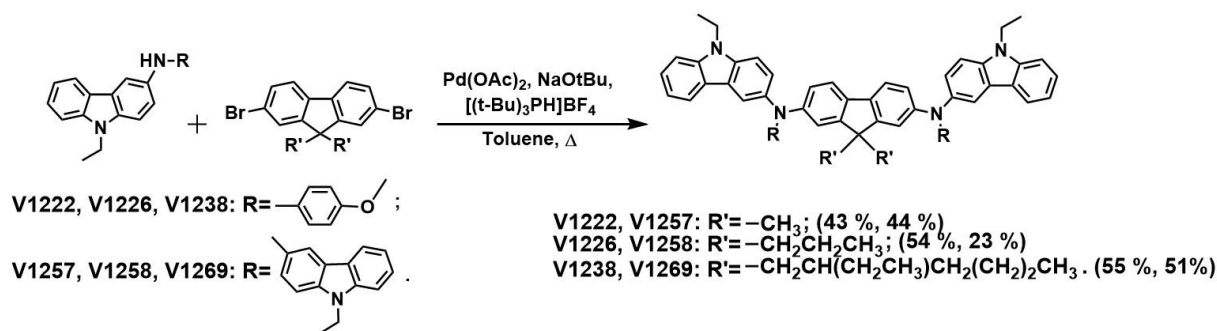
Scheme 2. Synthesis of the "half" compounds **V1222**, **V1226**, **V1238**, **V1257**, **V1258**, and **V1269**.

2.2. Optical properties

To investigate optical properties of the synthesized compounds, ultraviolet–visible (UV/vis) and photoluminescence (PL) spectra of the respective solutions in tetrahydrofuran (THF) were recorded. In **Figure 1** comparison between Spiro-OMeTAD, **V1240** and **V1267** are presented.
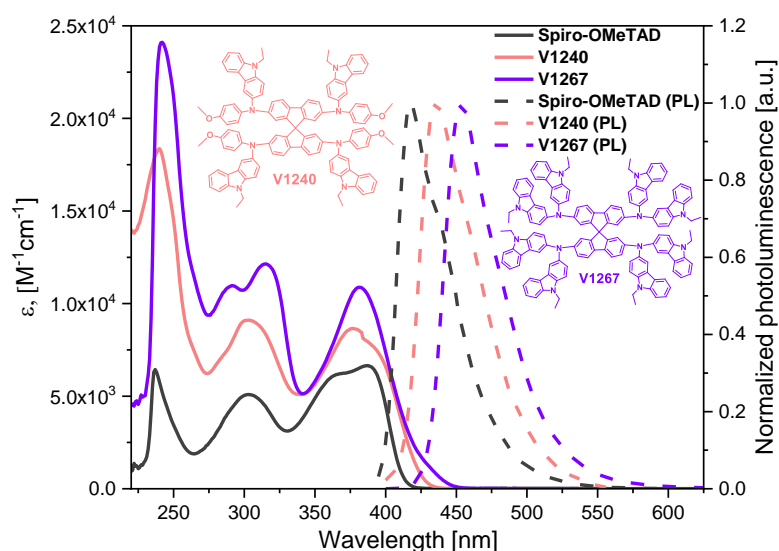

Figure 1. UV/Vis absorption (solid lines) and normalized PL (dashed line) spectra, recorded from the THF solutions of the 9,9′-spirobifluorene-based HTMs: **V1240**, **V1267**, and Spiro-OMeTAD (UV/vis - 10^{-4} м; PL - 10^{-5} м).

As it can be seen, the overall shape of the spectra of the new materials is similar to that of the Spiro-OMeTAD, inclining that only minor changes are induced by the change of the methoxyphenyl moieties for carbazolyl chromophores. With the growing number of carbazole units an increasement of absorption intensity (hyperchromic effect) can be observed, especially in the region around 250 nm, where absorption is dominant by that of the transitions in the heterocyclic systems. On the other hand, in the PL spectra a significant red shift is observed (Spiro-OMeTAD – 417 nm, **V1240** – 435 nm, **V1267** – 453 nm), suggesting higher relaxation due to the vibrational and/or rotational motions in carbazole moieties.

The "half" compounds exhibited roughly two times lower UV/vis absorption intensity with the overall shape matching that of the 9,9′-spirobifluorene-based analogue (**Figure 2**). This result could be expected, as the different number of methoxyphenyl and(or) carbazolyl chromophores in the molecules does not influence conjugation in the HTM structures.
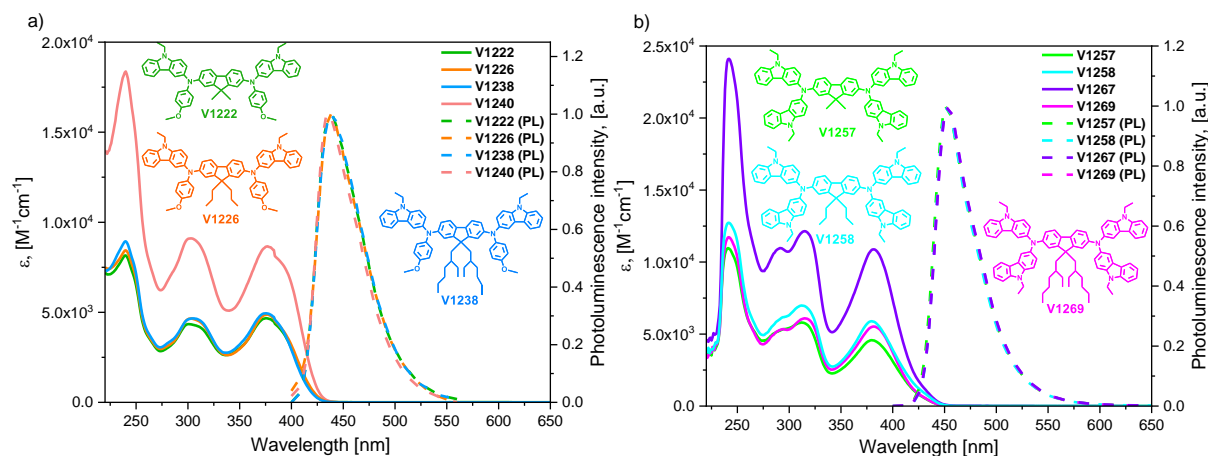

Figure 2. UV/Vis absorption (solid lines) and normalized PL (dashed lines) spectra, recorded from THF solutions of the HTMs: a) **V1222**, **V1226**, **V1238**, and **V1240** with 9-ethyl-*N*-(4-metoxyphenyl)-9*H*-carbazol-3-yl-amine fragments and b) **V1257**, **V1258**, **V1267**, **V1269** with bis(9-ethyl-9*H*-carbazol-3-yl)amine chromophores (UV/vis - 10^{-4} м; PL - 10^{-5} м).

2.2. Thermal properties

To evaluate thermal behavior of new HTMs, thermogravimetric analysis (TGA) and differential scanning calorimetry (DSC) measurements were performed. **Table 1** and **Figure S1** reveal the parameters of thermal behavior of new synthesized compounds, as well as that of the reference material Spiro-OMeTAD. Overall, all new compounds are stable up to 400 °C, which is much higher than operating temperatures of the solar cells (~ 60 °C).[33] Comparing TGA analysis data of new spirobifluorene class compounds with Spiro-OMeTAD it can be noted that replacement of four methoxyphenyl substituents by carbazolyl fragments slightly decreases T_d (Spiro-OMeTAD T_d = 449 °C,[34] **V1240** T_d = 438 °C), while T_d increases by 63 °C when all methoxyphenyl fragments are substituted by carbazolyl moieties (**V1267** T_d = 512 °C).

For the "half" compounds with two carbazolyl moieties T_d values are in the range of 401–452 °C with lower value observed for the material **V1238** possessing longest aliphatic chain. HTMs with four carbazolyl fragments in general have shown higher T_d values in the range of 461–515 °C. Interestingly, in this case compound **V1269** with 2-ethylhexyl aliphatic chains has shown the highest T_d, suggesting that there are significant differences in the packing of the molecules. Comparing these "half" compounds groups with each other, it is evident that incorporation

of carbazolyl fragments into molecule increases T_d.

The glass transition temperatures (T_g) of all new compounds are given in **Table 1** and **Figures S2–S3**. Both new spirobifluorene-based compounds **V1240** and **V1267** have shown higher T_g (169 °C and 139 °C respectively) in comparison with Spiro-OMeTAD (124 °C), what can be explained by increased molecular weight.

Table 1. Thermal and photophysical properties of the synthesized compounds

Compound	T_g,[a] [°C]	T_d,[b] [°C]	E_{ox}, [eV]	I_p, [eV]	μ_0, [cm²·(V·s)⁻¹] (E_0 = 0 V/cm),	μ, [cm²·(V·s)⁻¹] (E = 6.4·10⁵ V/cm)	σ, [S·cm⁻¹]
			9,9′-Spirobifluorene-based compounds				
Spiro-OMeTAD[34]	124 (T_m=245 °C)[c]	449	-0.05	5.0	4.1·10⁻⁵	5.0·10⁻⁴	3.01·10⁻⁴
V1240	169	438	-0.08	5.28	5.6·10⁻⁶ [d]	8.8·10⁻⁴ [d]	2.60·10⁻⁴
V1267	139	512	-0.17	4.90	3.6·10⁻⁴ [d]	1.6·10⁻³ [d]	6.96·10⁻⁴
			Fluorene-based "half" molecules with methoxyphenyl and carbazolyl chromophores				
V1222	147	452	-0.07	4.93	3.9·10⁻⁴ [d]	3.1·10⁻² [d]	4.63·10⁻⁴
V1226	133	441	-0.07	4.95	3.8·10⁻⁵ [d]	1.9·10⁻³ [d]	3.51·10⁻⁴
V1238	77	401	-0.08	5.02	1.8·10⁻⁵	5.3·10⁻⁴	3.28·10⁻⁵
			Fluorene-based "half" molecules with carbazolyl chromophores				
V1257	196	490	-0.15	4.85	3.6·10⁻⁵ [d]	1.6·10⁻³ [d]	1.94·10⁻⁴
V1258	183	461	-0.15	4.85	1.2·10⁻⁵ [d]	1.2·10⁻³ [d]	2.68·10⁻⁴
V1269	127	515	-0.15	4.96	3·10⁻⁵ [d]	2.9·10⁻⁴ [d]	1.98·10⁻⁴

[a] Glass transition temperature, extracted from the second DSC heating cycle;

[b] Decomposition temperature, corresponding to the 5% weight loss;

[c] Melting point (T_m) was not detected for all of the new compounds;

[d] The values of the hole drift mobility were evaluated by extrapolation of the results, obtained from the measurements of the mixture of the HTMs with PC-Z polymer binder.

Comparison of T_g of the "half" compounds revealed that materials with longer side chains showed lower T_g values. Overall, T_g of the compounds with both methoxyphenyl and carbazolyl chromophores (**V1222**, **V1226**, and **V1238**) was lower by ~50 °C compared to that of the respective analogues with only carbazolyl chromophores (**V1257**, **V1258**, and **V1269**). The reason behind this could be lower symmetry of the first group of compounds. The lowest T_g of 77 °C in case of compound **V1238** could negatively affect the long-term stability of the devices,[34] but all the other HTMs showed T_g significantly exceeding 100 °C.

In addition, it is important to note, that melting process was not observed for all of new synthesized compounds, indicating that they have only an amorphous state, what is an advantage for the formation of homogenous films, thus eliminating possibility for films to crystallize during operation of the devices.

2.3. Electrical properties

To evaluate energy levels of new HTMs, their oxidation potential (E_{ox}) in the solution and solid-state ionization potential (I_p) values were measured by means of cyclic voltammetry (CV) and photoelectron spectroscopy in air (PESA) techniques respectively. The results are presented in **Table 1** and **Figures S5, S6**. It is evident from the CV measurements that upon the introduction of carbazole moiety material can be more readily oxidized, therefore compounds, in which all methoxyphenyl fragments have been substituted by carbazolyl, exhibit lower E_{ox} values. Other changes in the structures have almost no impact on E_{ox} values. Similar trend is observed for I_p values, however in this case the variation in values for the compounds with the same chromophores is larger, suggesting some influence of packing in the bulk. In both cases, the values obtained for spiro-compounds are somewhat larger, than that of the corresponding "half" molecules. Overall, all synthesized HTMs are compatible with perovskite absorber materials values of the energy levels.

The ability of new HTMs to transport charges was evaluated by the xerographic time of flight (XTOF) technique, and measured hole drift mobility (μ_0 and μ) values are presented in **Table 1** and **Figure S4**. Some of materials can not be measured from pure layers, therefore, to obtain more durable layers, the samples were mixed with bisphenol Z-polycarbonate (PC-Z) additive. As a general trend, it can be seen that introduction of longer aliphatic chains has a negative impact for the ability to transport charges, which can be attributed to increased influence of the insulating fragments. "Half" compounds have higher mobility values for the series of compounds with both, methoxyphenyl and carbazolyl chromophores. However, different situation is observed for spiro compounds, where HTM **V1240** have demonstrated lower values, in comparison to that of **V1267**. Such difference might be attributed to the differences in the packing, occurring due to presence of the spiro core in the structure. Nevertheless, all synthesized compounds are showing transporting abilities sufficient for their application in PSCs.

Thin-film photoluminescence measurements were performed to analyse the hole extraction capability of different HTMs. The perovskite and perovskite/HTM layers were prepared on glass and excited at a wavelength of 625 nm from the perovskite or HTM side, respectively. The corresponding spectra is presented in **Figure 3** and the quenching effect provoked by the HTM was compared with the bare perovskite emission (**Table S1**). A significantly quenched emission is observed upon deposition of the HTMs on top of the bare perovskite layer, suggesting an efficient hole extraction. The samples containing fluorene-based "half" molecutes with carbazolyl or methoxyphenyl and carbazolyl units present a higher quenched emission than for spirobifluorene-based HTMs, suggesting a better hole-extracting capability.

The lateral conductivity of the different HTMs were measured with organic field-effect transistor (OFET) substrates (**Figure S7**) and the values are presented in **Table 1**. All HTMs present similar conductivity values with that of the Spiro-OMeTAD ($\sim 10^{-4}$ S·cm^{-1}) except of the **V1238**, which show the lowest value of studied HTMs with a conductivity of $3.28 \cdot 10^{-5}$ S·cm^{-1}.

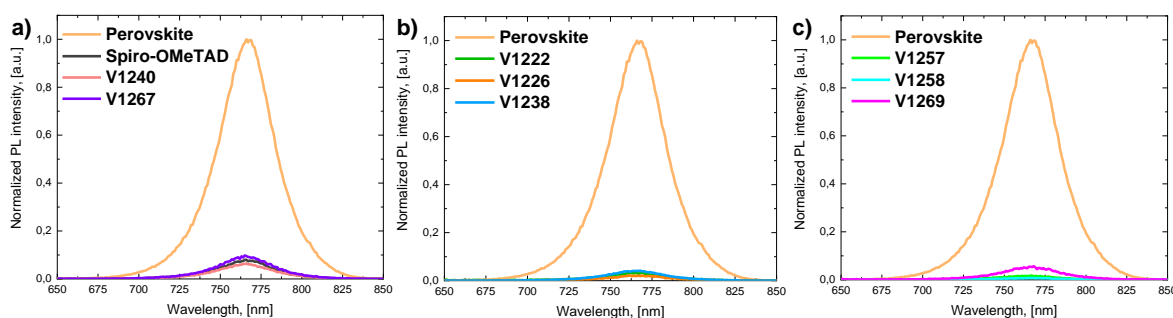**Figure 3.** PL spectra of perovskite and perovskite/HTM layers deposited on glass (λ_{exc}=625 nm). a) 9,9′-Spirobifluorene-based HTMs: Spiro-OMeTAD, **V1240** and **V1267**, b) Fluorene-based "half" molecules with methoxyphenyl and carbazolyl moieties: **V1222**, **V1226**, **V1238** and c) Fluorene-based "half" molecules with carbazolyl moieties: **V1257**, **V1258** and **V1269**.

2.4. Performance in Solar Cells

Solution-processed *n-i-p* perovskite solar cells were fabricated to investigate new compounds in comparison to the widely employed Spiro-OMeTAD. The device structure is: FTO/c-TiO$_2$/m-TiO$_2$/SnO$_2$/(FAPbI$_3$)$_{0.87}$(MAPbBr$_3$)$_{0.13}$]$_{0.92}$(CsPbI$_3$)$_{0.08}$/HTM/Au, where the HTM (20 mM in chlorobenzene) was doped with *tert*-butylpyridine (tBP), lithium tris(bis(trifluoromethylsulfonyl)imide) (LiTFSI) and tris(2-(1*H*-pyrazol-1-yl)-4-*tert*-(butylpyridine)cobalt(III) (CoTFSI, FK209). Further details on the device fabrication can be found in the Supporting Information.

The top-view and cross-sectional scanning electron microscopy (SEM) images (**Figures S8–S10**) demonstrate that the surface coverage of perovskite layer by the HTMs is complete and without presence of pin holes or aggregation.[35, 36] The best-performing solar cells employing new HTMs are presented in **Figures 4a–4c** and the corresponding PV parameters listed in **Table 2**.

The replacement of methoxyphenyl for carbazolyl in spirobifluorene-based HTMs lead to solar cells with lower performance than the devices containing the widely used Spiro-OMeTAD. A strong decrease in open circuit voltage (V_{OC}) values indicates higher recombination in the device presumably due to issues at the perovskite/HTM interface. Despite the low V_{OC} values,

the devices still lead to high power conversion efficiencies (PCEs) of 17.6% and 18.3% for **V1240** and **V1267**, respectively.

Table 2. PV parameters extracted from the corresponding *J-V* curves of the champion devices.

Compound	V_{OC}, [mV]	J_{SC}, [mA·cm^{-2}]	FF	PCE, [%]
9,9′-Spirobifluorene-based materials				
Spiro-OMeTAD	1108	23.60	0.77	20.1
V1240	1000	22.32	0.79	17.6
V1267	1059	23.41	0.74	18.3
Fluorene-based "half" molecules with methoxyphenyl and carbazolyl chromophores				
V1222	1014	22.80	0.68	15.7
V1226	992	22.89	0.69	15.7
V1238	987	22.35	0.73	16.1
Fluorene-based "half" molecules with carbazolyl chromophores				
V1257	1034	23.37	0.71	17.2
V1258	1045	23.32	0.73	17.8
V1269	1048	23.35	0.74	18.1

For the devices fabricated with "half" fluorene-based HTMs, the solar cells containing carbazolyl chromophores present higher device performance that their equivalent one formed with methoxyphenyl and carbazolyl units. The lower PV performance of the devices with methoxyphenyl and carbazolyl-based HTMs cannot be attributed to issues in the electronic properties of the molecules (see **Table 1**).
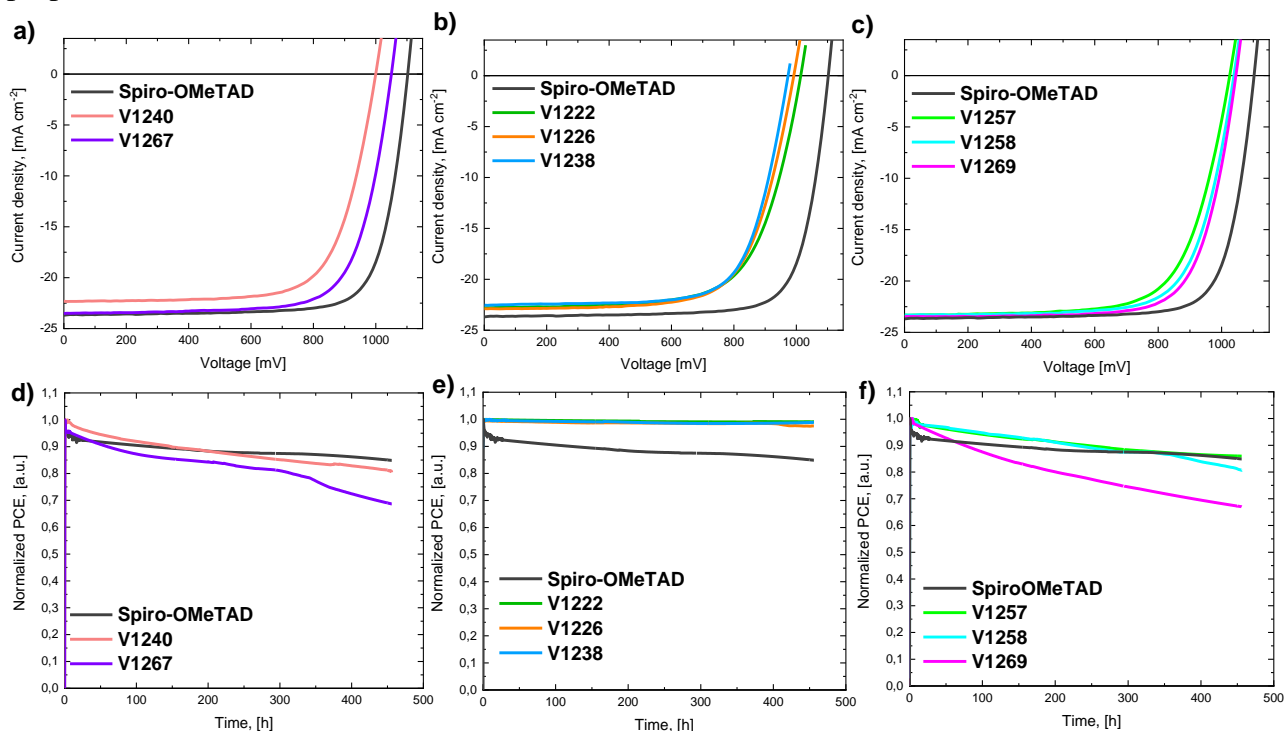

9

Figure 4. *J-V* curves and long-term stability of the most efficient solar cells containing a,d) Spiro-OMeTAD, **V1240** and **V1267** HTMs, b,e**) V1222**, **V1226** and **V1238** HTMs and c,f) **V1257**, **V1258** and **V1269** HTMs. The stability test was performed in unencapsulated devices kept in N$_2$ atmosphere at 25°C.

Therefore, the lower performance in methoxyphenyl and carbazolyl-devices might be originated by a poorer perovskite/HTM interface than for perovskite/carbazolyl-HTM one. As previously observed,[30] the increasing alkyl chain length does not influence on the short-circuit current density values of the devices as the values are almost identical (22.4–22.8 mA cm^{-2} for methoxyphenyl and carbazolyl-HTM and 22.3 mA cm^{-2} for carbazolyl-HTMs). The device performance is enhanced at increasing alkyl chain length due to higher fill factor (FF) values. The corresponding external quantum efficiency (EQE) of the devices are presented in **Figure S11**.

The long-term stability of the devices was evaluated in unencapsulated device under continuous 1 sun illumination in N$_2$ atmosphere at 25°C (see **Figures 4d–4f**). The devices containing spirobifluorene-based materials present a continuous decrease of PCE, in accordance with other reported long-term stability of devices containing Spiro-OMeTAD, achieving 85% (Spiro-OMeTAD), 81% (**V1240**) or 69% (**V1267**) of its maximum efficiency under 450 h operation. Similar behaviors are observed for devices containing fluorene-based "half" molecules with carbazolyl chromophores with efficiency decays of 86, 81 or 67% for **V1257**, **V1258** and **V1269**, respectively, after 450 h illumination. On the contrary, devices containing HTM with methoxyphenyl and carbazolyl units (**V1222**, **V1226**, **V1238**) presents with almost no degradation after 450 h under continuous illumination.

Water contact angles of the HTMs film coated on glass substrate were measured to better understand their humidity stability (Fig. S12). The water contact angle increase with the extension of alkyl side chains in the 9,9-positions of the central fluorene fragment in the "half" structures, from 81°, 80° (**V1222**, **V1257**) and 86°, 87° (**V1226**, **V1258**) to 90° (**V1238**, **V1269**), while the smallest contact angle of 72° was obtained by Spiro-OMeTAD analogous **V1267** possessing the carbazolyl chromophores. In addition, the hydrophobicity of the other Spiro-OMeTAD analogous **V1240** possessing the methoxyphenyl and carbazolyl increases (82°) and is higher than as Spiro-OMeTAD (77°). The trend of the contact angle is broadly in line with the results of the stability results.

3. Conclusion

In summary, we present the synthesis of the series of novel Spiro-OMeTAD analogues with the simple "half" structures and a systematic study of the impact of a terminated photoconductive chromophore on thermal, optical, photophysical, and photovoltaic properties. Molecular engineering of new hole transporting materials was realized under Hartwig-Buchwald amination conditions using commercially available starting materials. New compounds bear alkylated fluorene and spirobifluorene fragments as molecule-core, while 9-ethyl-*N*-(4-metoxyphenyl)-9*H*-carbazol-3-amine and bis(9-ethyl-9*H*-carbazol-3-yl)amine were used to build side chromophores. All synthesized HTMs exhibit excellent thermal stability, which depends on alkyl chain length and the number of carbazolyl moieties, at up to 400 °C. Additionally, these compounds are amorphous having an advantage of the ability to form homogenous films, and further eliminating possibility for films to crystallize during operation of the devices. The PCE of the most efficient n-i-p PSCs perovskite devices containing carbazolyl-terminated Spiro-OMeTAD analogue **V1267** has reached 18.3 %, and thus outperform the devices fabricated using the other HTMs: **V1269** (18.1 %), **V1258** (17.8 %), **V1240** (17.6 %), **V1257** (17.21 %), **V1238** (16.1 %), **V1226** (15.7 %), **V1222** (15.7 %). Furthermore, "half" structures with methoxyphenyl/carbazolyl fragments show excellent long-term stability and outperform Spiro-OMeTAD. We believe that this study offers a facile approach for developing new HTMs that can influence the PSC performance *via* molecular engineering of the side chromophores of the fluorene-based HTMs.

Supporting Information

Supporting Information is available from the Wiley Online Library or from the author.

References

[1]   A. Kojima, K. Teshima, Y. Shirai, T. Miyasaka, *J. Am. Chem. Soc.* **2009**, *131*, 6050.

[2]   https://www.nrel.gov/pv/cell-efficiency.html, accessed 09-**2021**.

[3]   A. Al-Ashouri, E. Köhnen, B. Li, A. Magomedov, H. Hempel, P. Caprioglio, J. A. Márquez, A. B. Morales Vilches, E. Kasparavicius, J. A. Smith, N. Phung, D. Menzel, M. Grischek, L. Kegelmann, D. Skroblin, C. Gollwitzer, T. Malinauskas, M. Jošt, G. Matič, B. Rech, R. Schlatmann, M. Topič, L. Korte, A. Abate, B. Stannowski, D. Neher, M. Stolterfoht, T. Unold, V. Getautis, S. Albrecht, *Science* **2020**, *370*, 1300.

[4]   F. Mathies, E. J. W. List-Kratochvil, E. L. Unger, *Energy Technol.* **2020**, *8*, 1900991.

[5]   J. Li, J. Dagar, O. Shargaieva, M. A. Flatken, H. Köbler, M. Fenske, C. Schultz, B. Stegemann, J. Just, D. M. Többens, A. Abate, R. Munir, E. Unger, *Adv. Energy Mater.* **2021**, *11*, 2003460.

[6]   M. Ernst, J. P. Herterich, C. Margenfeld, M. Kohlstädt, U. Würfel, *Sol. RRL* **2021**, 2100535.

[7]   J. Ávila, C. Momblona, P. P. Boix, M. Sessolo, H. J. Bolink, *Joule* **2017**, *1*, 431.

[8]   M. Roß, L. Gil-Escrig, A. Al-Ashouri, P. Tockhorn, M. Jošt, B. Rech, S. Albrecht, *ACS Appl. Mater. Interfaces* **2020**, *12*, 39261.

[9]   Z. Li, J. Li, H. Cao, Y. Qian, J. Zhai, Y. Qiu, L. Yang, S. Yin, *ACS Appl. Mater. Interfaces* **2021**, *13*, 45496.

[10]   P. Roy, N. K. Sinha, S. Tiwari, A. Khare, *Solar Energy* **2020**, *198*, 665.

[11]   M. Saliba, J. P. Correa-Baena, C. M. Wolff, M. Stolterfoht, N. Phung, S. Albrecht, D. Neher, A. Abate, *Chem. Mater.* **2018**, *30*, 4193.

[12]   N. J. Jeon, J. H. Noh, Y. C. Kim, W. S. Yang, S. Ryu, S. I. Seok, *Nature Mater* **2014**, *13*, 897.

[13]   M. Saliba, T. Matsui, J. Y. Seo, K. Domanski, J. P. Correa-Baena, M. K. Nazeeruddin, S. M. Zakeeruddin, W. Tress, A. Abate, A. Hagfeldt, M. Grätzel, *Energy Environ. Sci.* **2016**, *9*, 1989.

[14]   M. Stolterfoht, C. M. Wolff, J. A. Márquez, S. Zhang, C. J. Hages, D. Rothhardt, S. Albrecht, P. L. Burn, P. Meredith, T. Unold, D. Neher, *Nat Energy* **2018**, *3*, 847.

[15]   L. Calió, S. Kazim, M. Grätzel, S. Ahmad, *Angew. Chem. Int. Ed.* **2016**, *55*, 14522.

[16]   Z. Shariatinia, *Renewable and Sustainable Energy Reviews* **2020**, *119*, 109608.

[17]   C. H. Teh, R. Daik, E. L. Lim, C. C. Yap, M. A. Ibrahim, N. A. Ludin, K. Sopian, M. A. M. Teridi, *J. Mater. Chem. A* **2016**, *4*, 15788.

[18]   J. Lian, B. Lu, F. Niu, P. Zeng, X. Zhan, *Small Methods* **2018**, *2*, 1800082.

[19]   X. Tong, F. Lin, J. Wu, Z. M. Wang, *Adv. Sci.* **2016**, *3*, 1500201.

[20]   B. Li, Y. Cai, X. Tian, X. Liang, D. Li, Z. Zhang, S. Wang, K. Guo, Z. Liu, *Journal of Energy Chemistry* **2021**, *62*, 523.

[21]   S. Yang, H. Zhao, M. Wu, S. Yuan, Y. Han, Z. Liu, K. Guo, S. (F.) Liu, S. Yang, H. Zhao, S. Yuan, Y. Han, Z. Liu, S. Liu, M. Wu, K. Guo, *Solar Energy Materials and Solar Cells* **2019**, *201*, 110052.

[22]   M. Wu, J. Li, R. Zhang, X. Tian, Z. Han, X. Lu, K. Guo, Z. Liu, Z. Wang, *Org. Lett*. **2018**, *20*, 780.

[23]   K. Guo, M. Wu, S. Yang, Z. Wang, J. Li, X. Liang, F. Zhang, Z. Liu, Z. Wang, *Solar RRL*, **2019**, *3*,1800352.

[24]   T. Braukyla, R. Xia, M. Daskeviciene, T. Malinauskas, A. Gruodis, V. Jankauskas, Z. Fei, C. Momblona, C. Roldan-Carmona, P. J. Dyson, V. Getautis, M. K. Nazeeruddin, *Angew. Chem. Int. Ed*.**2019**,*58*,11266.

[25]   X. Liu, S. Ma, M. Mateen, P. Shi, C. Liu, Y. Ding, M. Cai, M. Guli, M. K. Nazeeruddin, S. Dai, *Sustainable Energy Fuels* **2020**, *4*, 1875.

[26]   K. Rakstys, S. Paek, A. Drevilkauskaite, H. Kanda, S. Daskeviciute, N. Shibayama, M. Daskeviciene, A. Gruodis, E. Kamarauskas, V. Jankauskas, V. Getautis**,** M. K. Nazeeruddin, *ACS Appl. Mater. Interfaces* **2020**, *12*, 19710.

[27]   C. Hao, X. Zong, Y. Cheng, M. Zhao, M. Luo, Y. Zhang, S. Xue, *Sustainable Energy Fuels* **2021**, *5*, 5548.

[28]   T. Qin, F. Wu, L. Zhu, W. Chi, Y. Zhang, Z. Yang, J. Zhao, Z. Chi, *Organic Electronics* **2022**, *100*, online, DOI: 10.1016/j.orgel.2021.106325.

[29]   D. Y. Lee, G. Sivakumar, Manju, R. Misra, S. I. Seok**,** *ACS Appl. Mater. Interfaces* **2020**, *12*, 28246.

[30]   S. Daskeviciute, C. Momblona, K. Rakstys, A. A. Sutanto, M. Daskeviciene, V. Jankauskas, A. Gruodis, G. Bubniene, V. Getautis, M. K. Nazeeruddin, *J. Mater. Chem. A* **2021**, *9*, 301.

[31]   N. J. Jeon, H. Na, E. H. Jung, T. Y. Yang, Y. G. Lee, G. Kim, H. W. Shin, S. I. Seok, J. Lee, J. Seo, *Nat. Energy* **2018**, *3*, 682.

[32]   J. Wang, H. Zhang, B. Wu, Z. Wang, Z. Sun, S. Xue, Y. Wu, A. Hagfeldt, M. Liang,

Angew. Chem., Int. Ed. **2019**, *58*, 15721.

[33]   E. Aydin, T. G. Allen, M. De Bastiani, L. Xu, J. Ávila, M. Salvador, E. Van Kerschaver, S. De Wolf, *Nat. Energy* **2020**, *5*, 851.

[34]   T. Malinauskas, D. Tomkute-Luksiene, R. R. Sens, M. Daskeviciene, R. Send, H. Wonneberger, V. Jankauskas, I. Bruder, V. Getautis, *ACS Appl. Mater. Interfaces* **2015**, *7*, 11107.

[35]   J. Y. Feng, K. W. Lai, Y. S. Shiue, A. Singh, C. H. P. Kumar, C. T. Li, W. T. Wu, J. T. Lin, C. W. Chu, C. C. Chang, C. Su, *J. Mater. Chem. A* **2019**, *7*, 14209.

[36]   X. C. Li, Y. G. Tu, C. Meng, W. Song, T. Cheng, Y. T. Gong, J. Min, R. Zhu, W. Y. Lai, W. Huang, *ACS Appl. Mater. Interfaces* **2019**, *11*, 45717.